J. Astron. Space Sci. 25(4), 375–382 (2008)

Earthward Flow Bursts in the Magnetotail Driven by Solar Wind Pressure Impulse

Khan-Hyuk Kim†, Young-Sil Kwak, Jae-Jin Lee, and Junga Hwang
Korea Astronomy and Space Science Institute, 61-1, Hwaam-dong, Yuseong-gu, Daejeon 305-348, Korea
email: khan@kasi.re.kr

(Received August 18, 2008; Accepted October 8, 2008)

Abstract

On August 31, 2001, $\sim$ 1705 – 1718 UT, Cluster was located near the midnight magnetotail, GSE (x, y, z) $\sim$ $(-19, -2, 2)$ RE, and observed fast earthward flow bursts in the vicinity of the neutral sheet. They occurred while the tail magnetic field suddenly increased. Using simultaneous measurements in the solar wind, at geosynchronous orbit, and on the ground, it is confirmed that tail magnetic field enhancement is due to an increased solar wind pressure. In the neutral sheet region, strongly enhanced earthward flow bursts perpendicular to the local magnetic field ($V_{\perp x}$) were observed. Auroral brightenings localized in the pre-midnight sector ($\sim$ 2200 – 2400 MLT) occurred during the interval of the $V_{\perp x}$ enhancements. The $V_{\perp x}$ bursts started $\sim$ 2 minutes before the onset of auroral brightenings. Our observations suggest that the earthward flow bursts are associated with tail reconnection directly driven by a solar wind pressure impulse and that $V_{\perp x}$ caused localized auroral brightenings.

Keywords: substorm, solar wind pressure impulse, magnetotail

1. Introduction

Magnetic reconnection in the near-earth region of the magnetotail is one of main processes for magnetotail dynamics. Accelerated earthward and tailward plasma flows within the near-tail plasma sheet have been usually taken as evidence for reconnection (e.g., Nagai et al. 1998). Fast flows in the central plasma sheet are mostly earthward at $X_{GSM} > -20\ R_E$ (e.g., Baumjohann et al. 1989, Angelopoulos et al. 1992). This indicates that the neutral line usually forms tailward beyond $\sim$ 20 R_E.

Although many studies of fast flows in the earth's magnetotail have been reported, there are few observations of earthward flow bursts directly triggered by external source (solar wind pressure impulse) to the authors' knowledge. In this paper we report on observations of earthward flow bursts triggered by solar wind pressure impulse. They were observed in the vicinity of the central plasma sheet by Cluster. The flow bursts occurred while the tail magnetic field suddenly increased. We will show that the enhanced magnetic field is due to the solar wind pressure increase.

2. Observations

Figures 1a and 1b show the solar wind dynamic pressure (nMV^2), the interplanetary magnetic field (IMF) B_z in GSE (geocentric solar ecliptic) coordinates, and the magnitude of IMF (dotted

†corresponding author

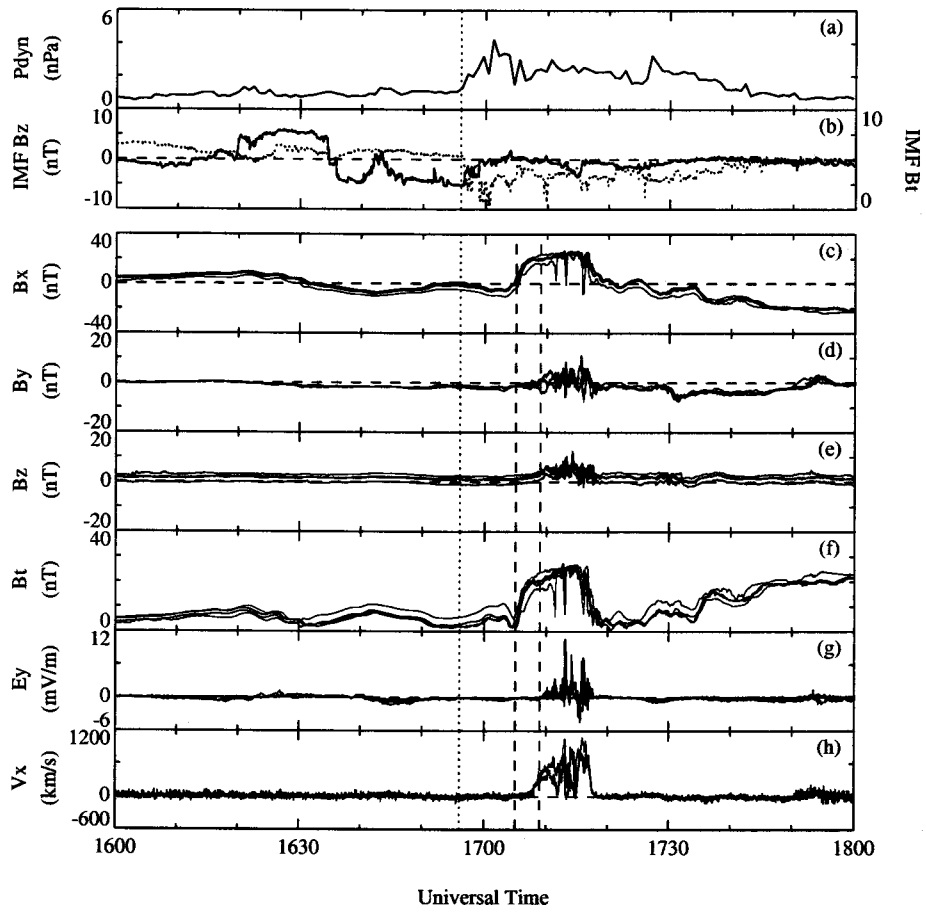

Figure 1. (a) Solar wind dynamic pressure from Geotail; (b) IMF B_z (solid line) and the magnitude of the IMF (dotted line) from Geotail; (c)-(h) Spin (~4 s) averaged magnetic field, y component of electric field, x component of plasma flow data in GSE coordinates from Cluster (black is spacecraft 1, red is spacecraft 2, green is spacecraft 3, and blue is spacecraft 4).

line) observed by Geotail from 1600 to 1800 UT on August 31, 2001. The resolutions of the Geotail plasma (Frank et al. 1994) and magnetic field (Kokubun et al. 1994) data are ~50 s and ~3 s, respectively. During the 2-hour interval Geotail was near the Sun-Earth line and moved from GSE (x, y, z) ~ (29.1, 0.2, 2.1) to (29.5, 1.3, 2.3) R_E. The solar wind speed (not shown) was ~400-480 km/s for this interval. The solar wind dynamic pressure suddenly increased at 1656 UT (marked by the vertical dotted line), and northward turning of IMF occurred at the time.

During the interval from 1600 to 1800 UT, Cluster was near the midnight magnetotail, GSE (x, y, z) ~ $(-19, -2, 2)$ R_E. Figures 1c-1h show the magnetic field, the y component of the electric field, and the x component of the plasma flow in GSE coordinates from Cluster spacecraft. Detailed descriptions of magnetic field (FGM), electric field (EFW), and plasma (CIS) measurements are given by Balogh et al. (2001), Gustafsson et al. (1997), and Reme et al. (2001), respectively. The

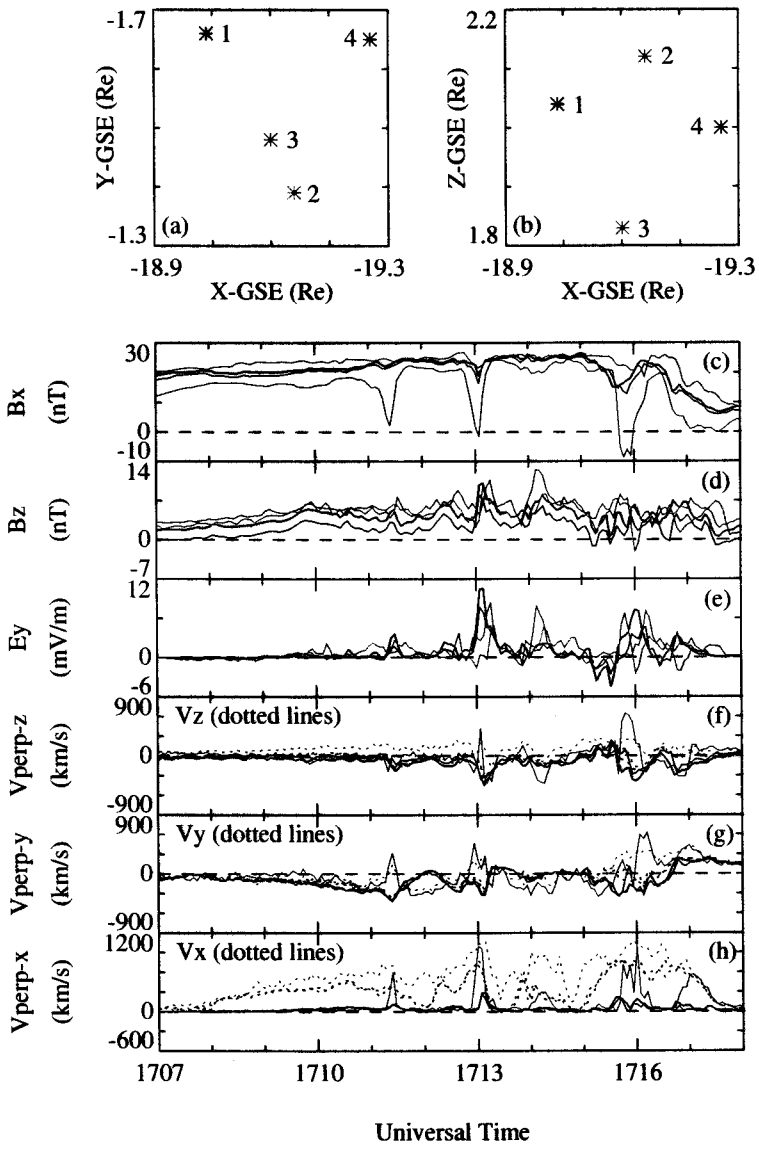

Figure 2. Locations of the Cluster spacecraft at 1713 UT in GSE x-y (a) and x-z (b) planes; (c)-(h) The magnetic field, electric field, and plasma flows (black is spacecraft 1, red is spacecraft 2, green is spacecraft 3, and blue is spacecraft 4).

four Cluster spacecraft are plotted with black, red, green, and blue to represent spacecraft 1, 2, 3, and 4. Note that the CIS data for spacecraft 2 are not available for the interval in our study. We will show below that spacecraft 3 was located closest to the ecliptic plane (i.e., GSE x-y plane) while spacecraft 2 was located farthest from the ecliptic plane.

The total magnetic field strength was as low as ~10 nT for the interval of 1600-1705 UT. This indicates that Cluster was close to the neutral sheet. During this time interval, E_y and V_x were weak and quiet. Cluster crossed a very quiet neutral sheet from the north to the south around at 1630 UT. The sequence of the passage of the neutral sheet past the four spacecraft was spacecraft 3 (green), 4 (blue), 1 (black), and then 2 (red). During the time intervals, ~1630-1705 and ~1720-1800 UT (~1600-1630 and ~1705-1720 UT), the magnetic field strength at spacecraft 3 was larger (smaller) than that at other spacecraft, indicating that the magnetic field gradient is directed along Z_{GSE}. That is, spacecraft 3 was located farthest from (closest to) the neutral sheet for the intervals, ~1630-1705 and ~1720-1800 UT (~1600-1630 and ~1705-1720 UT).

Cluster observed a rapid increase in the magnetic field intensity at around 1705 UT (marked by the vertical dashed line). For the interval from ~1705 to ~1718 UT, the magnetic field strength increased to more than ~20 nT. This is mainly due to the increase in B_x. If the magnetic field enhancement at Cluster is caused by the solar wind pressure impulse at 1656 UT, the time delay of 9 min from Geotail to Cluster can be estimated using a solar wind speed of 470 km/s, a nominal magnetosheath speed of 200 km/s, a subsolar point of the bow shock at 15 R_E and of the magnetopause at 10 R_E, and the fast mode propagation speed of 1000 km/s inside the magnetosphere (e.g., Moore et al. 1987). We note that the fast mode speed varies greatly in the magnetosphere. Thus, the propagation speed inside the magnetosphere should be considered as an averaged value.

The enhancement in the tail magnetic field strength could be due to the increased solar wind pressure which squeezes the magnetotail as it moves tailward. If the tail magnetic field directly responds to an increase in solar wind lateral pressure, the magnetosheath flow speed should be considered for a time delay. Assuming 80% of the solar wind speed in the magnetosheath around the flank magnetopause (Spreiter et al. 1966), the propagation time of the pressure impulse from Geotail to Cluster will be ~13 min. The vertical dashed line at 1709 UT indicates the time of the magnetotail compression responding to the solar wind lateral pressure.

Large earthward flow bursts beginning at around 1708 UT were observed. The flow speed was larger at spacecraft 3 than at spacecraft 1 and 4. Spacecraft 3 observed flow velocity exceeding 1000 km/s. The flow bursts were accompanied by large field fluctuations in B_y, B_z, and E_y. They had a duration of about 10 min and disappeared as the strength of total magnetic field decreased. These observations suggest that the flow bursts are associated with the magnetotail compression. The field and flow variations will be examined in more detail below in the expanded time scale.

Figures 2a and 2b show the locations of the Cluster spacecraft at 1713 UT in GSE coordinates. B_x, B_z, and E_y are plotted in Figures 2c-2e. Figures 2f-2h plot plasma flows (dotted line) and plasma flows perpendicular to the magnetic field (solid lines). Vector quantities in Figure 2 are in GSE coordinates. Spacecraft 3, located closest to the neutral sheet, observed sharply decreased Bx magnetic field with amplitude of 2.0, –1.57, and –8.7 nT at 1711:24, 1713:04, and 1715:48 UT, respectively. However, B_x at the other spacecraft was about 20 nT. This implies that the current sheet transiently moved upward near spacecraft 3 and was crossed by spacecraft 3 at 1713:04 and 1715:48 UT. Spacecraft 3 and 4 were separated by ~1200 km in GSE z. Thus, the current sheet thickness was less than ~1200 km. This thin current sheet is comparable to that from recent observations (Runov et al. 2003).

The enhanced E_y perturbations were in phase with the B_z perturbations and out of phase with $V_{\perp z}$ except for when spacecraft 3 was in the southern hemisphere in close vicinity of the neutral sheet at ~1715:50 UT. Note that $V_\perp$ in our study indicates plasma flow perpendicular to the local magnetic field. At that time, E_y enhancement was in phase with $V_{\perp z}$. This indicates that E_y corresponds not only to earthward transport of northward field lines but also to southward (northward) transport of B_x in the northern (southern) hemisphere. The earthward fast flows beginning around

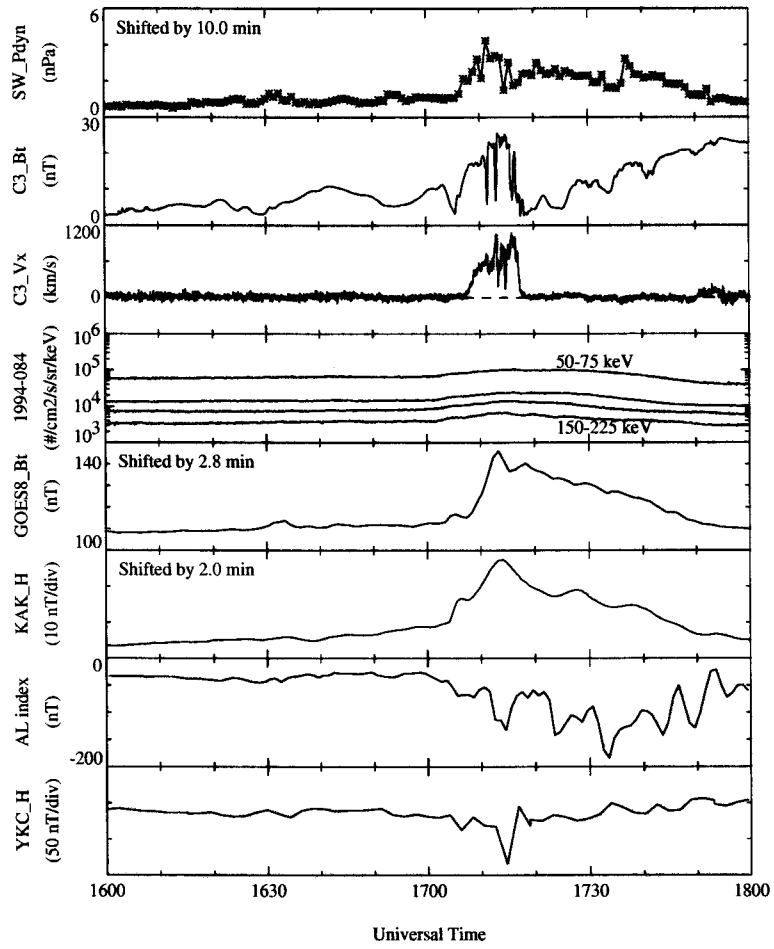

Figure 3. Time-shifted solar wind pressure, magnetic field strength and V_x at Cluster (spacecraft 3), LANL energetic electron data (50-225 keV), time-shifted magnetic field strength at GOES 8, time-shifted Kakioka H, AL index, and Yellowknife H.

1708 UT were largely in the field aligned component. The plasma flow variations at spacecraft 1 and 4 were very similar each other, but significantly different from those at spacecraft 3. This indicates that the plasma flows are largely variable along the Y and Z axes in the vicinity of the neutral sheet. Large perpendicular earthward flows were observed as spacecraft 3 entered the neutral sheet region. They were accompanied by B_z increase and B_x decrease, that is, local magnetotail magnetic field dipolarization. These field variations during the $V_{\perp z}$ bursts at 1711:24, 1713:04, 1714:10, 1716, and 1717 UT are very similar to those during the bursty bulk flow (BBF) in the inner central plasma sheet discussed by Angelopoulos et al. (1992). Thus, $V_{\perp z}$ bursts in our study can be categorized as the BBFs. The flow direction in V_y ($V_{\perp y}$) was changed from dawnward to duskward in the neutral sheet region.

Figure 3 shows the solar wind dynamic pressure at Geotail, the total magnetic field strength and

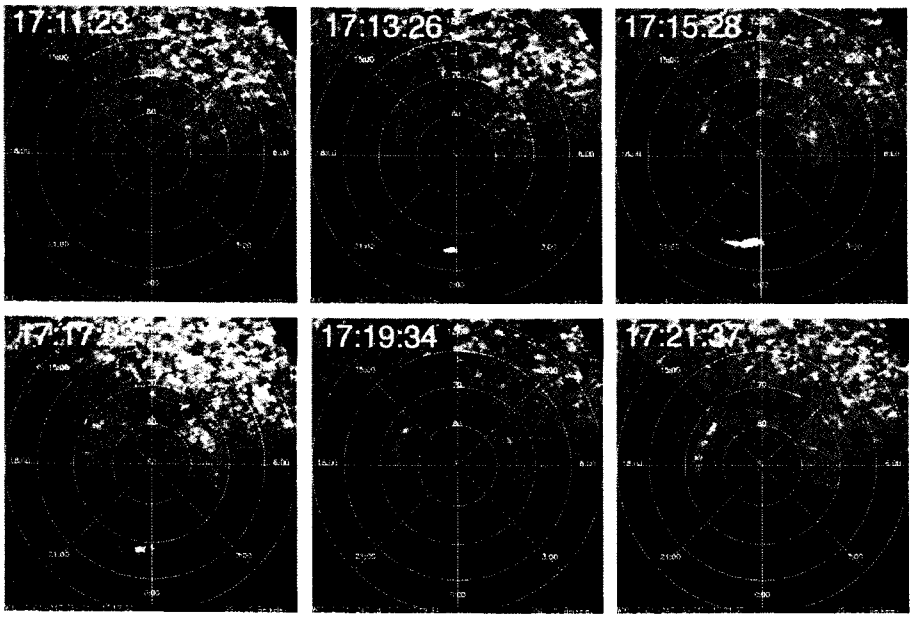

Figure 4. A sequence of IMAGE WIC far ultraviolet images.

V_x at spacecraft 3 of Cluster, the energetic electrons (50-225 keV) from the Los Alamos 1994-084 spacecraft (local time = UT+6.9 hours), the total magnetic field strength at the geostationary GOES 8 satellite (local time = UT?5.0 hours), the magnetic field H (northward) component of the low-latitude Kakioka (KAK) ground station (local time = UT+9.3 hours, L ~ 1.25), the AL index, and Yellowknife (YKC, local time = UT+16.3 hours) H component, which is one of AE stations. The solar wind dynamic pressure from Geotail has been shifted by a constant time delay of 10.0 min. The GOES 8 and KAK data have been lagged by 2.8 min and 2.0 min, respectively, assuming the propagation speed of 1000 km/s inside the magnetosphere. During the 2-hour interval, GOES 8 was located near the subsolar region while KAK was post-midnight.

The magnetospheric compression caused by the solar wind discontinuity is clearly seen in the total magnetic field strength at GOES 8. Its shape is very similar to that in the H component at KAK. This implies that the increased H at KAK is due to the magnetospheric compression. After considering the propagation delays, the sudden increases in the solar wind pressure, in the total magnetic field at GOES 8, and in the H component at KAK coincide well with the magnetic field and V_x enhancements at Cluster. 1994-084 spacecraft was located near the midnight at 1700 UT and observed no substorm injection. However, there are gradual electron flux increases during the interval (~1700-1750 UT) of the increase in the magnetic field strength at GOES 8. These flux variations may be due to a global magnetospheric response to solar wind dynamic pressure variations. The AL index fluctuated around −100 nT for the interval ~1710-1800 UT. AL sharply decreased around 1711 UT. This signature was also observed at YKC on the morningside (~0900 LT). The AL fluctuations from 1720 to 1800 UT were out of phase with those at YKC. These observations suggest that the AL variations may be due to magnetospheric compression by the solar wind pressure variations

(Kokubun et al. 1977).

Figure 4 shows a series of 6 auroral images, from 1711:23 to 1721:37 UT, observed with IMAGE Wideband Imaging Camera (WIC) experiment (Mende et al. 2000). Each image is plotted in a MLT-magnetic latitude coordinate system. At 1713:26 UT sudden auroral brightening was observed ant it lasted until ~1718 UT. Dramatic brightening occurred at 1715:28 UT. The auroral enhancement was localized around 2200-2400 MLT. The auroral brightenings at 1713:26 and 1715:28 UT are ~2 min after the earthward $V_{\perp x}$ bursts at 1711:24 and 1713:04 UT developed. Strong auroral brightening at 1715:28 UT may be due to fast earthward $V_{\perp x}$ flow exceeding 1000 km/s at 1713:04 UT. This suggests that auroral enhancements are associated with $V_{\perp x}$ bursts (Fairfield et al. 1999).

3. Summary

Cluster observed very quiet V_x variations near the central plasma sheet before the solar wind pressure impulse passed. During the passage of the solar wind pressure impulse, the tail magnetic field suddenly increased and fast earthward V_x bursts were observed near the midnight meridian at radial distance of 19 R_E. Such flows in the plasma sheet have been considered to be a signature of reconnection taking place beyond the satellite location. Since Cluster was near the central plasma sheet, the increase in the tail magnetic field during the passage of the solar wind pressure impulse suggests that the plasma sheet was thinning. The thinning is associated with an enhancement of the cross-tail current caused by stretched tail magnetic fields. If the vertical component of magnetic field across the plasma sheet becomes very small (i.e., the tail magnetic field becomes very stretched), magnetic reconnection can be initiated in the central plasma sheet (Coroniti 1985, Baker & McPherron 1990). Thus, our observations suggest that the V_x bursts are directly driven by the solar wind pressure impulse. That is, tail reconnection is triggered by external force.

It has been suggested that the plasma sheet thinning is associated with a substorm energy storage phase (i.e., substorm growth phase) prior to substorm expansion phase onset and that the energetic particle flux decrease (or dropout) occurs near the end of the growth phase (e.g., Baker & McPherron 1990). In our study, however, we observed no particle flux dropout and injection at the geosynchronous orbit near the midnight. Well-defined Pi2 signatures (not shown) were not observed at the low-latitude KAK station during the interval of the fast earthward flows. These observations suggest that the fast earthward flows associated with tail reconnection triggered by external force do not develop substorm.

Localized auroral brightening in the premidnight sector (2200-2400 MLT) occurred during the interval of the earthward $V_{\perp x}$ and duskward $V_{\perp y}$ bursts in the neutral sheet region. The onset of the $V_{\perp x}$ and $V_{\perp y}$ bursts was observed ~2 min before auroral enhancements. These observations indicate that the near-earth reconnection began prior to the auroral enhancement (Ohtani et al. 1999, Baker et al. 2002). The auroral brightening lasted a few minutes without particle flux dropout and injection at geosynchronous orbit. Thus, the auroral event is similar to pseudobreakup (Akasofu 1964).

Acknowledgements: We thank L. Frank at University of Iowa for the Geotail CPI data. The Geotail magnetic field data were provided through DARTS at the Institute of Space and Astronautical Science (ISAS) in Japan. The Cluster data were provided by the Space Physics Data Facility (SPDF). We would like to thank A. Balogh and E. Lucek for Cluster magnetic field data, H. Reme for Cluster plasma data, and G. Gustafsson for Cluster electric field data. We would like to thank S. B. Mende for making the auroral images from IMAGE/WIC available. The energetic particle data were provided by G. D. Reeves through Los Alamos Energetic Particle home page of LANL geosynchronous

spacecraft. The AL index, KAK, and YKC magnetometer data were provided by World Data Center C2 for Geomagnetism, Kyoto University.

References

Akasofu, S.-I. 1964, Planet. Space Sci., 12, 273

Angelopoulos, V., Kennel, C. F., Coroniti, F. V., Pellat, R., Kivelson, M. G., Walker, R. J., Baumjohann, W., & Luhr, H. 1992, JGR, 97, 4027

Baker, D. N. & McPherron, R. L. 1990, JGR, 95, 6591

Baker, D. N., Peterson, W. K., Eriksson, S., Li, X., Blake, J. B., Burch, J. L., Daly, P. W., Dunlop, M. W., Korth, A., Donovan, W., Friedel, R., Fritz, T. A., Frey, H. U., Mense, S. B., Roeder, J., & Singer, H. J. 2002, GRL, 29, 2190, doi:10.1029/2002GL015539

Balogh, A., Carr, C. M., Acuna, M. H., Dunlop, M. W., Beek, T. J., Brown, P., Fornacon, K.-H., Georgescu, E., Glassmeier, K.-H., Harris, J., Musmann, G., Oddy, T., & Schwingenschuh, K. 2001, Ann. Geophys., 19, 1207

Baumjohann, W., Paschmann, G. & Cattell, C. A. 1989, JGR, 94, 6597

Coroniti, F. V. 1985, JGR, 90, 7427

Fairfield, D. H., Mukai, T., Reeves, G. D., Kokubun, S., Parks, G. K., Nagai, T., Matsumoto, H., Hashimoto, K., Gurnett, D. A., & Yamamoto, T. 1999, JGR, 104, 355

Frank, L. A., Ackerson, K. L., Paterson, W. R., Lee, J. A., English, M. R., & Pickett, G. L. 1994, J. Geomag. Geoelectr., 46, 23

Gustafsson, G., Bostrom, R., Holback, B., Holmgren, G., Lundgren, A., Stasiewicz, K., Ahlen, L., Mozer, F. S., Pankow, D., Harvey, P., Berg, P., Ulrich, R., Pedersen, A., Schmidt, R., Butler, A., Fransen, A. W. C., Klinge, D., Thomsen, M., Falthammar, C.-G., Lindqvist, P.-A., Christenson, S., Holtet, J., Lybekk, B., Sten, T. A., Tanskanen, P., Lappalainen, K., and Wygant, J. 1997, Space Sci. Rev., 79, 137

Kokubun, S., MaPherron, R. L., & Russell, C. T. 1977, JGR, 97, 17177

Kokubun, S., Yamamoto, T., Acuna, M. H., Hayashi, K., Shiokawa, K., & Kawano, K. 1994, J. Geomag. Geoelectr., 46, 7

Mende, S. B., Heetderks, H., Frey, H. U., Lampton, M., Geller, S. P., Abiad, R., Siegmund, O. H. W., Tremsin, A. S., Spann, J., Dougani, H., Fuselier, S. A., Magoncelli, A. L., Bumala, S., Murphree, S., & Trondsen, T. 2000, Space Sci. Rev., 91, 287

Moore, T. E., Gallagher, D., Horwitz, J., & Comfort, R. 1987, GRL, 14, 1007

Nagai, T., Fujimoto, M., Saito, Y., Machida, S., Terasawa, T., Nakamura, R., Yamamoto, T., Mukai, T., Nishida, A., & Kokubun, S. 1998, JGR, 103, 4419

Ohtani, S., Creutzberg, F., Mukasi, T., Singer, H., Lui, A. T., Nakamura, M., Prikryl, P., Yumoto, K., & Rostoker, G. 1999, JGR, 104, 22713

Reme, H., et al. 2001, Ann. Geophys., 19, 1303

Runov, A., Nakamura, R., Baumjohann, W., Treumann, R. A., Zhang, T. L., Volwerk, M., Voros, Z., Balogh, A., Glasmeier, K.-H., Klecker, B., Reme, H., & Kistler, L. 2003, GRL, 30, 1579, doi:10.1029/2002GL016730

Spreiter, J. R., Summers, A. L., & Alksne, A. Y. 1966, Planet. Space Sci., 14, 223